UNSTEADY VISCOUS FLOW OVER PROLATE SPHEROIDS

R. S. Alassar*, H. Badr, A. Al-Rabeh, and R. Allayla

King Fahd University of Petroleum and Minerals
Dhahran, Saudi Arabia

Dedicated to the late Professor A. Al-Rabeh

الخلاصة :

تَمَّ في هذا البحث استخدام طريقة المتتاليات المقطوعة شبة التحليلية لحل معادلات ناڤير وستوكس الكاملة والتي تحكم السريان المفاجيء على جسم شبة كروي. فبعد كتابة المعادلات في متغيرات حالتي السريان والدوران، تم تمديد المتغيرات بمتتاليات ليجندرا. وقد تم حل المعادلات التفاضلية الناتجة بطريقة عددية. وتَعْرِضُ النتائجُ في هذا البحث أشكالَ التماثلِ لدالة الدوران بالإضافة إلى توزيع الضغط والدوان السطحي على شكل خطوط السريان. كما أننا نعرض للمتغيرات الزمنية لمعامل السحب.

ABSTRACT

In this paper, the semi-analytical series truncation method is used to solve the full Navier–Stokes equations for the impulsively started flow over a prolate spheroid. The equations are written in terms of the stream function and vorticity which are expanded in terms of series of Legendre functions. The resulting time-dependent differential equations are solved numerically. Results are presented in the form of streamline and equi-vorticity patterns as well as pressure and surface vorticity distributions. The time development of the drag coefficient is also presented.

*Address for correspondence:
KFUPM Box 1620
King Fahd University of Petroleum & Minerals
Dhahran 31261
Saudi Arabia

UNSTEADY VISCOUS FLOW OVER PROLATE SPHEROIDS

INTRODUCTION

Flow over prolate spheroids has been studied by few researchers. Payne and Pell [1] studied the special case of steady Stokes flow over prolate spheroids and a formula for the viscous drag was obtained. This formula was modified by Breach [2] using the two classical methods, those of Stokes [3] and Oseen [4] for finding approximations to viscous streaming at low Reynolds numbers. Kanwal [5] and Lai and Mockros [6] solved the linearized Stokes equations for the case of oscillating flow over a prolate spheroid. Although the general solution of the Stokes stream function was obtained, Kanwal failed to determine the constants of integration. Lai and Mockros were able to perform the necessary calculations to obtain a formula for the drag on a spheroid executing general axial translatory accelerations. The impulsively started flow over a prolate spheroid of 0.5 axis ratio was studied by Chang *et al.* [7] using the method of matched asymptotic expansion at small time and a hybrid vortex method for large time values. The range of Reynolds numbers (according to their definition) was from 100 to 6000.

The previously mentioned solutions, except for the work of Chang *et al.*, are valid at very low Reynolds numbers because of the considerable effects imposed by the non-linear inertia terms in the equations when dealing with flows at higher Reynolds numbers. In this paper, the time dependent full Navier–Stokes equations for unsteady axisymmetric flow over a prolate spheroid having an axis ratio of 0.6 for Reynolds numbers up to 20, are solved. The method of solution adopted is based on series truncation where the stream function and vorticity are expanded in terms of series of Legendre functions.

BASIC EQUATIONS AND METHOD OF SOLUTION

Consider a prolate spheroid, as shown in Figure 1, with major and minor axes of $2a$ and $2b$ placed in a viscous incompressible fluid of infinite extent which starts impulsively from rest. The Navier–Stokes equations for incompressible fluids can be written in vector notation as

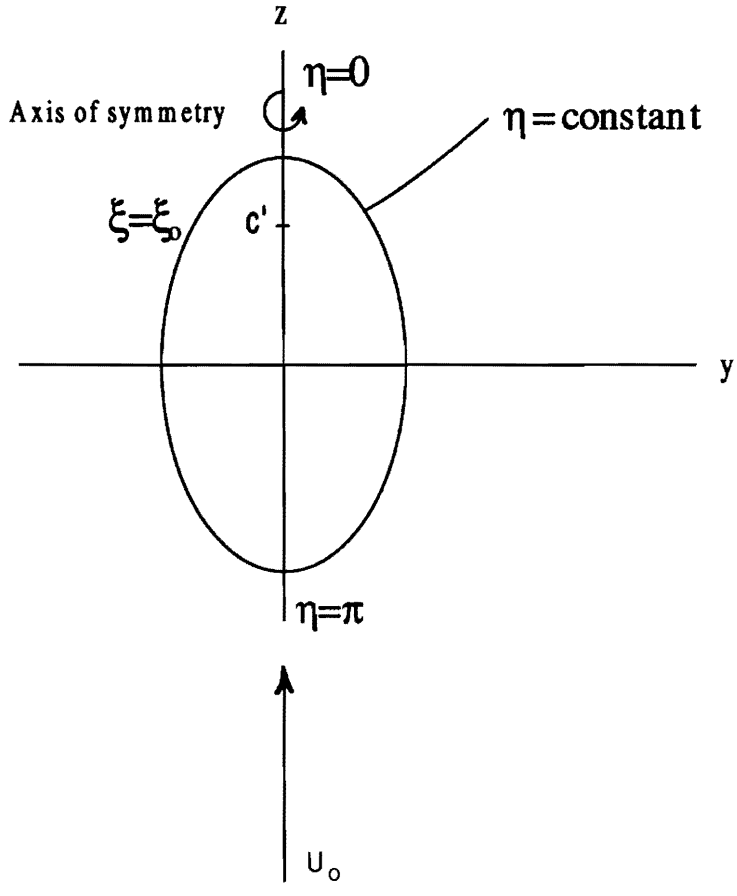

Figure 1.The Prolate Spheroidal Coordinate System.

$$\rho\left[\frac{\partial \vec{w}}{\partial t} + \left(\vec{w} \bullet \vec{\nabla}\right)\vec{w}\right] = \vec{\nabla}p + \vec{F} + \mu\vec{\nabla}^2\vec{w} \tag{1}$$

where, $\vec{w}$ is the velocity vector, ρ is the fluid density, $\vec{F}$ is the body force vector, p is the pressure in the fluid, t is time, and μ is the dynamic viscosity. The continuity equation for incompressible fluids is simply a zero divergence of the velocity vector,

$$\vec{\nabla} \bullet \vec{w} = 0. \tag{2}$$

The vorticity (ς) is defined in the usual way as the curl of the velocity vector.

$$\vec{\varsigma} = \vec{\nabla} \times \vec{w}. \tag{3}$$

If a stream function (ψ) is defined so that the continuity equation is satisfied, then its appropriate form is

$$h_2 h_3 w_1 = \frac{\partial \psi}{\partial q_2}, \qquad h_1 h_3 w_2 = -\frac{\partial \psi}{\partial q_1} \tag{4}$$

where q_1, q_2 are the space coordinates of the orthogonal curvilinear coordinate, and h_i are some scale factors. It should be noted that we strictly speak of axisymmetric or two-dimensional problems. The vorticity is then a scalar and a stream function is an appropriate definition.

The quantity $(\vec{w} \bullet \vec{\nabla})\vec{w}$ in Equation (1) is a pseudo-vector and can be expanded as:

$$\left(\vec{w} \bullet \vec{\nabla}\right)\vec{w} = \vec{\nabla}\left(w^2/2\right) - \vec{w} \times \left(\vec{\nabla} \times \vec{w}\right) \tag{5}$$

$$\text{and, } \vec{\nabla}^2\vec{w} = \vec{\nabla}\left(\vec{\nabla} \bullet \vec{w}\right) - \vec{\nabla} \times \left(\vec{\nabla} \times \vec{w}\right). \tag{6}$$

The prolate spheroidal coordinate system (ξ, η, ϕ) is related to the cartesian coordinate system by:

$$\begin{aligned} x &= c' \sinh\xi \sin\eta \cos\phi \\ y &= c' \sinh\xi \sin\eta \cos\phi \\ z &= c' \cosh\xi \cos\eta, \end{aligned} \tag{7}$$

with the corresponding scale factors given by:

$$h_\xi = h_\eta = c'\sqrt{\sinh^2\xi + \sin^2\eta} \qquad h_\phi = c' \sinh\xi \sin\eta. \tag{8}$$

Using these coordinate scale factors, the equations for the three-dimensional axisymmetric flow over prolate spheroids in terms of the stream function and vorticity can be written as:

$$\left(\sinh^2\xi + \sin^2\eta\right)\zeta + \frac{\partial}{\partial\xi}\left(\frac{1}{\sin\eta\sinh\xi}\frac{\partial\psi}{\partial\xi}\right) + \frac{\partial}{\partial\eta}\left(\frac{1}{\sin\eta\sinh\xi}\frac{\partial\psi}{\partial\eta}\right) = 0 \tag{9}$$

$$\left(\sinh^2\xi + \sin^2\eta\right)\frac{\partial\zeta}{\partial t} + \frac{\partial\psi}{\partial\eta}\frac{\partial}{\partial\xi}\left(\frac{\zeta}{\sinh\xi\sin\eta}\right) - \frac{\partial\psi}{\partial\xi}\frac{\partial}{\partial\eta}\left(\frac{\zeta}{\sinh\xi\sin\eta}\right) = \frac{2}{Re}\left\{\frac{\partial}{\partial\xi}\left[\frac{1}{\sinh\xi}\frac{\partial}{\partial\xi}(\sinh\xi\,\zeta)\right] + \frac{\partial}{\partial\eta}\left[\frac{1}{\sin\eta}\frac{\partial}{\partial\eta}(\sin\eta\,\zeta)\right]\right\}. \tag{10}$$

The variables in Equations (9) and (10) are dimensionless by the following expressions:

$\psi = \frac{\psi'}{U_o c'^2}, \zeta = \frac{\zeta' c'}{U_o}, t = \frac{t' U_o}{c'}, w = \frac{w'}{U_o}$, where c' is the focal distance, U_o is the free stream velocity. The Reynolds number is defined as $Re = \rho U_o(2c')/\mu$. All variables with primes are dimensional. The no-slip and impermeability conditions on the spheroid surface and the free stream conditions far away lead to the following boundary conditions:

$$\psi = \frac{\partial \psi}{\partial \eta} = \frac{\partial \psi}{\partial \xi} = 0 \quad \text{at } \xi = \xi_o \tag{11}$$

$$\frac{\partial \psi}{\partial \xi} = \frac{1}{2}\sinh 2\xi \sin^2 \eta, \text{ and } \quad \frac{\partial \psi}{\partial \eta} = \frac{1}{2}\sinh^2 \xi \sin 2\eta \quad \text{as } \xi \to \infty \tag{12}$$

$$\text{or, } \psi = \frac{1}{2}\sinh^2 \xi \sin^2 \eta \quad \text{as } \xi \to \infty, \tag{13}$$

where $\xi_o \left(\xi_o = \tanh^{-1} b/a\right)$ defines the surface of the prolate spheroid. The flow away from the prolate spheroid is irrotational leading to,

$$\zeta \to 0 \quad \text{as } \xi \to \infty. \tag{14}$$

Consider the following expansions for ψ and ζ:

$$\psi = \sum_{n=1}^{\infty} f_n(\xi, t) \int_{\omega}^{1} P_n(\tau)\, d\tau \tag{15}$$

$$\zeta = \sum_{n=1}^{\infty} g_n(\xi, t) P_n^1(\omega) \tag{16}$$

where $P_n(\omega)$ and $P_n^1(\omega)$ are the Legendre and first associated Legendre polynomials of order n respectively, and $\omega = \cos\eta$. These functions form a complete orthogonal set in the range $\omega = -1$ to $\omega = 1$. The method is an extension of that used by Dennis and Walker [8] for the sphere case. These series when substituted in Equations (9) and (10) and integrating over ω from -1 to 1 after multiplying by , $P_m^1(\omega)$, produce the following set of differential equations:

$$\begin{aligned} \frac{\partial^2 f_n}{\partial \xi^2} - \coth\xi \frac{\partial f_n}{\partial \xi} - n(n+1) f_n &= \sinh\xi\, n(n+1)\left[\cosh^2\xi - \frac{2n^2+2n-3}{(2n-1)(2n+3)}\right] g_n \\ &\quad - \sinh\xi \frac{n(n+1)(n+2)(n+3)}{(2n+3)(2n+5)} g_{n+2} + \sinh\xi \frac{n(n-1)(n-2)(n+1)}{(2n-1)(2n-3)} g_{n-2} \end{aligned} \tag{17}$$

$$\begin{aligned} &\left[\cosh^2\xi - \frac{2n^2+2n-3}{(2n-1)(2n+3)}\right]\frac{\partial g_n}{\partial t} - \frac{(n+2)(n+3)}{(2n+3)(2n+5)}\frac{\partial g_{n+2}}{\partial t} - \frac{(n-1)(n-2)}{(2n-1)(2n-3)}\frac{\partial g_{n-2}}{\partial t} \\ &\qquad = \frac{2}{Re}\left[\frac{\partial^2 g_n}{\partial \xi^2} + \coth\xi \frac{\partial g_n}{\partial \xi} - \left\{\frac{1}{\sinh^2\xi} + n(n+1)\right\} g_n\right] + S_n \end{aligned} \tag{18}$$

where,

$$S_n = -\frac{1}{\sinh\xi}\left[\sum_{i=1}^{\infty}\sum_{j=1}^{\infty} \alpha_{ij}^n f_i \left(\frac{\partial g_i}{\partial \xi} - \coth\xi_j\right) + \sum_{i=1}^{\infty}\sum_{j=1}^{\infty} \beta_{ij}^n g_j \frac{\partial f_i}{\partial \xi}\right] \tag{19}$$

where
$$\alpha_{ij}^{n} = -(2n+1)\sqrt{\frac{j(j+1)}{n(n+1)}}\begin{pmatrix} n & i & j \\ -1 & 0 & 1 \end{pmatrix}\begin{pmatrix} n & i & j \\ 0 & 0 & 0 \end{pmatrix} \tag{20}$$

and
$$\beta_{ij}^{n} = (2n+1)\sqrt{\frac{j(j^2-1)(j+2)}{n(n+1)i(i+1)}}\begin{pmatrix} n & i & j \\ -1 & -1 & 2 \end{pmatrix}\begin{pmatrix} n & i & j \\ 0 & 0 & 0 \end{pmatrix}; \tag{21}$$

$\begin{pmatrix} j_1 & j_2 & j_3 \\ m_1 & m_2 & m_3 \end{pmatrix}$ are the 3-j symbols. The boundary conditions can now be written with respect to the coefficient functions (modes) of the series as:

$$f_n(\xi_o, t) = \frac{\partial f_n}{\partial \xi}(\xi_o, t) = 0 \tag{22}$$

$$f_n(\xi, t) \to \sinh^2 \xi\, \delta_{n1} \quad \text{and} \quad g_n(\xi, t) \to 0 \quad \text{as} \quad \xi \to \infty. \tag{23}$$

No boundary conditions exist for the functions g_n on the surface of the spheroid. These values on the surface can be obtained through Equation (17) by approximating the space derivative $\partial^2 f_n/\partial \xi^2$ by second order accurate central differences.

Using the approximations (15) and (16), the independent space coordinates were reduced to only one coordinate (ξ). Consequently, the numerical difficulties and inaccuracy involved when obtaining derivatives with respect to the other coordinate (η) are avoided. Now, the solution of the original differential equations can be obtained by solving the differential equations corresponding to the modes of the truncated series. This can be accomplished by solving Equation (18) using a Crank–Nicolson finite-difference scheme. Equation (18) can be rewritten as:

$$S_1 \frac{\partial g_n}{\partial t} = S_2 \frac{\partial g_{n+2}}{\partial t} + S_3 \frac{\partial g_{n-2}}{\partial t} + q_n(\xi, t). \tag{24}$$

The quantities S_1, S_2, S_3, and q_n are easily identifiable. The Crank–Nicolson finite-difference approximation of Equation (24) results in:

$$\begin{aligned} \frac{S_1}{\Delta t}\left[g_n(\xi, t) - g_n(\xi, t-\Delta t)\right] = \frac{S_2}{\Delta t}\left[g_{n+2}(\xi, t) - g_{n+2}(\xi, t-\Delta t)\right] + \frac{S_3}{\Delta t}\left[g_{n-2}(\xi, t) - g_{n-2}(\xi, t-\Delta t)\right] \\ + \frac{1}{2}\left[q_n(\xi, t) + q_n(\xi, t-\Delta t)\right]. \end{aligned} \tag{25}$$

Using central differences for all derivatives in Equation (25) and rearranging, one obtains

$$A(\xi, t)g_n(\xi - \Delta\xi, t) + B(\xi, t)g_n(\xi, t) + C(\xi, t)g_n(\xi + \Delta\xi, t) = D(\xi, t-\Delta t) + E(\xi, t), \tag{26}$$

where $\Delta\xi$ is the step size, A, B, and C are easily identifiable functions of ξ that can be calculated at each mesh point, $D(\xi, t-\Delta t)$ is a completely known function, and $E(\xi, t)$ is a function that depends on the solution at time t. Equation (25), when applied at every mesh point, will result in a set of algebraic equations that forms a tridiagonal matrix problem which is solved for each value of n between 1 and N (N designates the number of terms taken in the series defined in Equations (15) and (16)) iteratively due to the dependence of the right hand side on values at time t and the appearance of the derivatives $\partial g_{n-2}/\partial t$ and $\partial g_{n+2}/\partial t$. Equation (17), on the other hand, is solved directly as a two-point boundary value problem. If central differences are used to approximate the space derivatives, a tridiagonal system is obtained which can be easily solved for the functions f_n. The numerical algorithm can be summarized as follows:

1. Determine the functions g_n at time t by sequentially solving the tridiagonal systems resulting from Equations (24) from $n = 1, N$. The known solution at time $(t - \Delta t)$ is used as an initial approximation for the functions g_n. For any value of n, the function g_{n-2} in Equation (24) is known and the value of g_{n+2} is initially approximated using the known solution at time $(t - \Delta t)$. That value is updated in the iterative-type solution when n is stepped up by 2.
2. After each mode g_n is determined, apply Equation (17) *on the surface of the spheroid* to obtain a better approximation for $g_n(\xi_o, t)$.
3. Obtain the functions $f_n(\xi, t)$ through the solution of Equation (17).
4. Go to step 1 and repeat the procedure until convergence is reached.
5. Increment time and repeat the whole procedure.

The condition set for convergence is $\left|g_n^{m+1}(\xi, t) - g_n^m(\xi, t)\right| < 10^{-5}$ where m denotes the iteration number. The number of iterations required for convergence is initially high (19 for the case $Re = 0.5$). At later times, only two to three iterations are necessary to pass to the next time step. Table 1 presents the first nine modes of the series on the surface of the spheroid. Very small time steps were initially used since the time variation of vorticity is quite fast. As time progresses, the time step was gradually increased. The time steps used were 0.001, 0.005, 0.01, and 0.02. The number of points in the ξ direction used varies with Reynolds number. At small Reynolds numbers, the flow is diffusive in nature and the vorticity extends far away into the bulk fluid. The mesh is adaptive which means that more points in the ξ direction are automatically considered when the far-value of the vorticity exceeds a certain tolerance. Table 2 compares the drag values at different lengths of the integration domain for the case $Re = 5$. The effect of the step size on the flow field near the spheroid was examined by comparing the results when using different values. A value of $h = 0.025$ was found satisfactory and was used for all cases. The total number of terms taken in the series depends on Reynolds number. The total number of terms was also determined automatically. When the last term (g_N) in the series exceeds 10^{-5}, one more term is added. High-Reynolds number cases require more terms. Figure 2 compares the surface vorticity for different number of terms (N) for the case $Re = 20$. Figure 3 presents the corresponding surface pressure distributions.

Table 1. Vorticity Modes on the Surface of the Spheroid.

Re	$g_1(\xi_o)$	$g_2(\xi_o)$	$g_3(\xi_o)$	$g_4(\xi_o)$	$g_5(\xi_o)$	$g_6(\xi_o)$	$g_7(\xi_o)$	$g_8(\xi_o)$	$g_9(\xi_o)$
5.0	2.2699	−0.3748	0.2799	−0.0635	0.0527	−0.0125	0.011	−0.0026	0.0023
10.0	2.6403	−0.6045	0.3170	−0.1037	0.0606	−0.0206	0.0126	−0.0042	0.0026
20.0	3.1750	−0.9573	0.3869	−0.1653	0.0748	−0.0332	0.0156	−0.0071	−0.0034

Table 2. Drag Coefficient at Different Lengths of Integration Domain for $Re = 5$.

Number of points in ξ direction	C_D
120	5.1644
140	5.1438
160	5.1393
180	5.1383

RESULTS & DISCUSSION

We define a drag coefficient C_D which relates the drag forces D on the spheroid to the dynamic head and the projected area of the spheroid $A\left(= \pi c'^2 \sinh^2 \xi_o\right)$ as:

$$C_D = \frac{D}{\rho U_o^2 A}. \tag{27}$$

By integrating the elementary friction and pressure forces over the entire surface, one can prove that C_{DF} (drag coefficient due to friction) and C_{DP} (drag coefficient due to pressure) are related to the functions $g_n(\xi, t)$ by:

$$C_{DF} = \frac{16 \coth \xi_o}{3Re} g_1(\xi_o, t) \tag{28}$$

$$C_{DP} = -\frac{8}{3Re}\left[\coth \xi_o \, g_1(\xi_o, t) + \frac{\partial g_1}{\partial \xi}(\xi_o, t)\right] \tag{29}$$

where, $C_D = C_{DF} + C_{DP}$. The dimensionless pressure $p^*(\eta, t)$ is defined as:

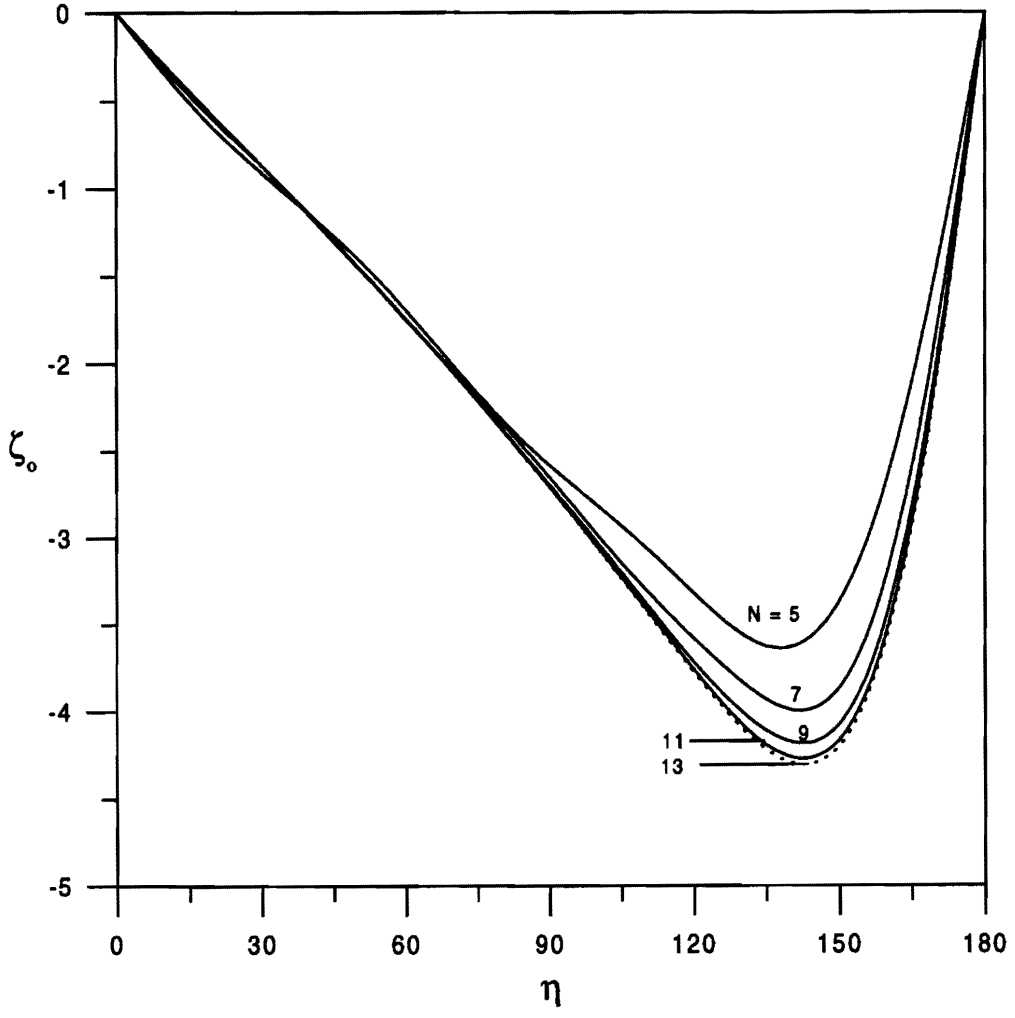

Figure 2. Surface Vorticity for Different Number of Terms in the Series.

$$p^*(\eta, t) = \frac{p'_n - p'_\pi}{1/2\rho U_o^2} \tag{30}$$

where p' is the dimensional pressure. By using the η-component of the Navier–Stokes equations, one can show that the surface pressure distribution is related to the vorticity distribution by:

$$p^*(\eta, t) = \frac{4}{Re}\sum_{n=1}^{N}\left[P_n(\cos\eta) - (-1)^n\right]\left[\frac{\partial g_n}{\partial \xi}(\xi_o, t) + \coth\xi_o\, g_n(\xi_o, t)\right]. \tag{31}$$

In order to verify the mathematical model and the computational scheme, we use the analytical formulas for C_D obtained by Payne and Pell [1] and by Breach [2] as a base for comparisons. These formulas were based on the solution of the steady linearized Stokes equations for the case of a prolate spheroid in an infinite fluid. Table 3 shows a good agreement between the present study and these formulas at low Re with a percentage difference not exceeding 2.5% at Re = 0.1. At higher Reynolds numbers (Re = 1.0), the difference reaches 11% for the Payne & Pell formula and reaches 9% for the Breach formula. This large difference is attributed to the non-linear inertia terms effect, which increases in magnitude with the increase of Re. We verify the present method of solution further by comparing with the results of Chang *et al.* [7]. The

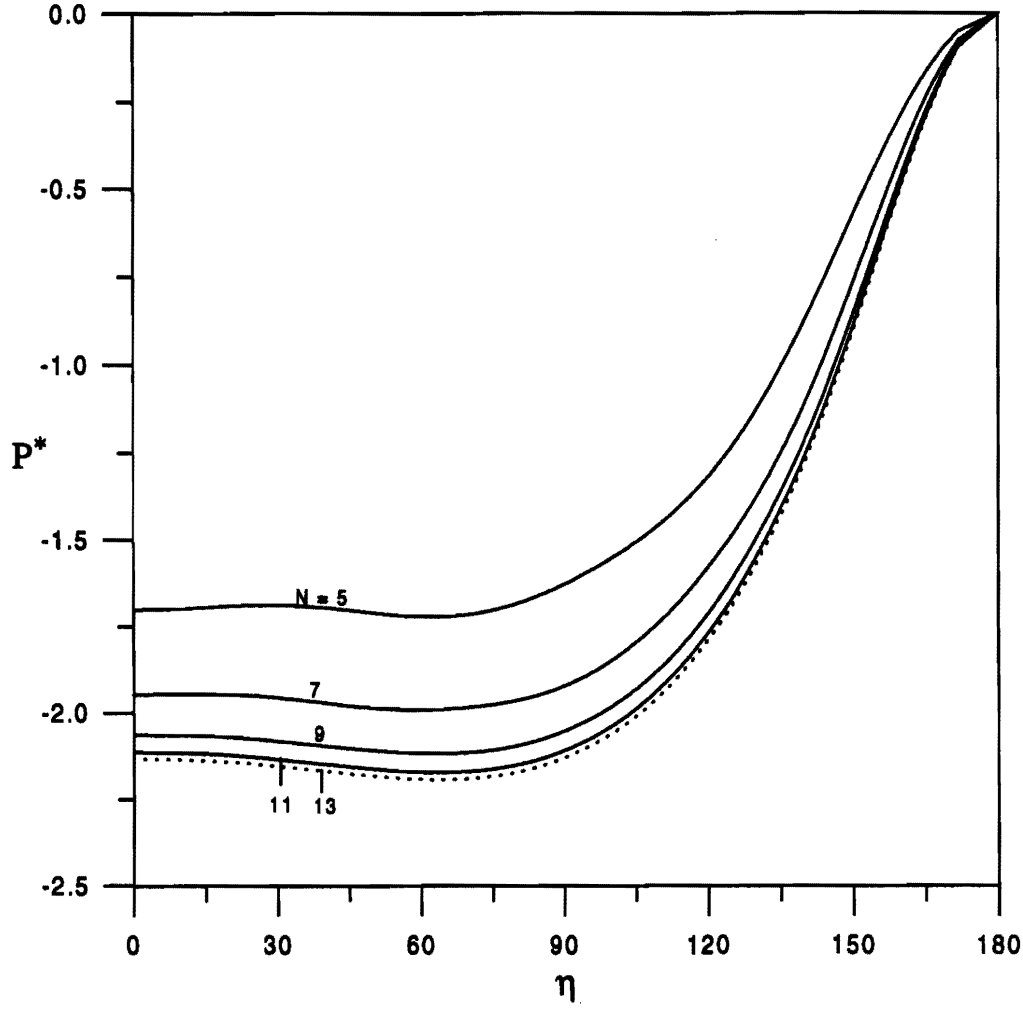

Figure 3. Dimensionless Pressure for Different Number of Terms in the Series.

values C_D, and C_{DF} obtained for the case $Re = 86.6$ (100) and $b/a = 0.5$ are respectively 0.888, and 0.694 which compare well with those obtained by Chang *et al.* (0.92(0.46), and 0.712(0.356)). It should be noted that these values are in accordance with the definitions of *Re* and drag coefficients in the present study. The values corresponding to Chang *et al.* definitions are between brackets. The difference between the present solution and that of Chang ranges between 2.5% and 3.2% which is attributed mainly to the difference in the solution methodology.

Table 3. Comparisons of Drag Coefficents.

Re	C_D present	C_D Payne & Pell [1]	C_D Breach [2]
0.1	186.300	181.731	182.198
0.5	39.077	36.346	36.806
1.0	20.473	18.173	18.633

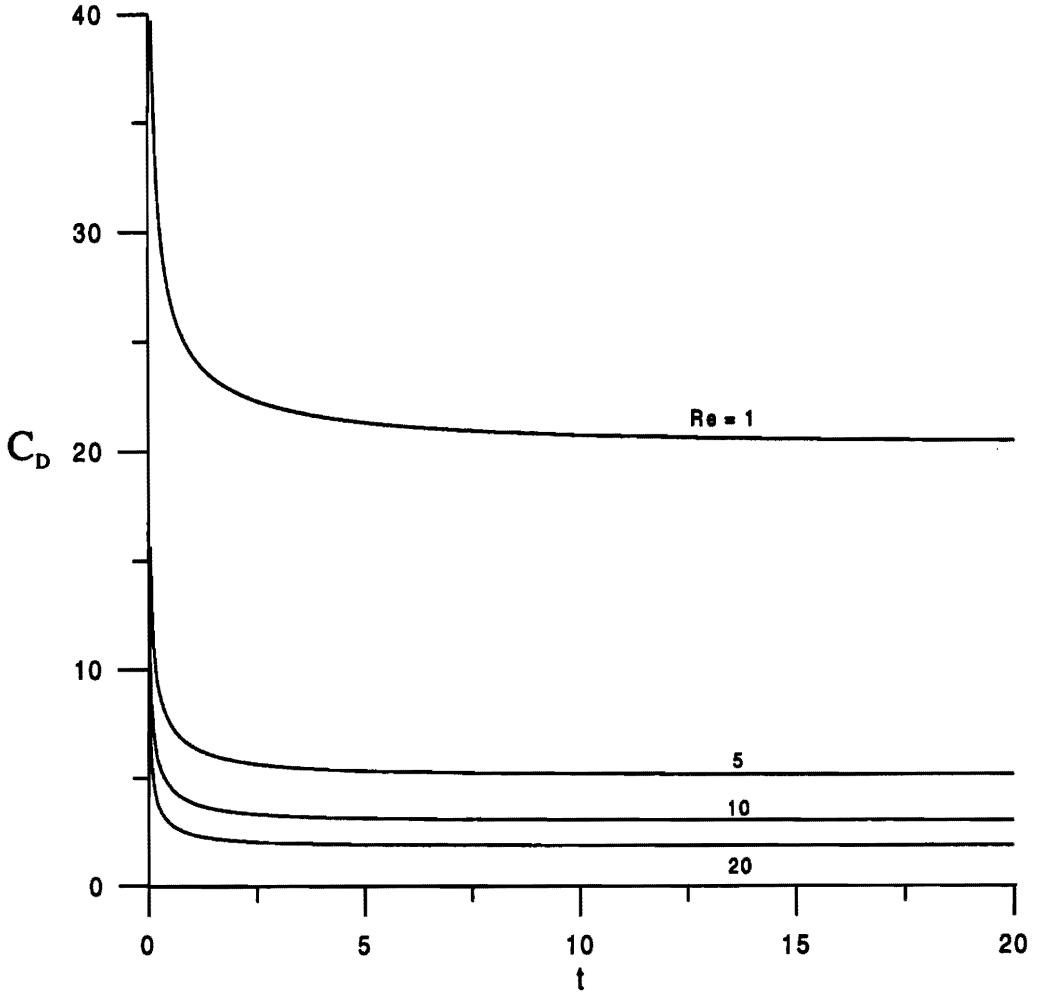

Figure 4. The Time Development of the Total Drag Coefficient.

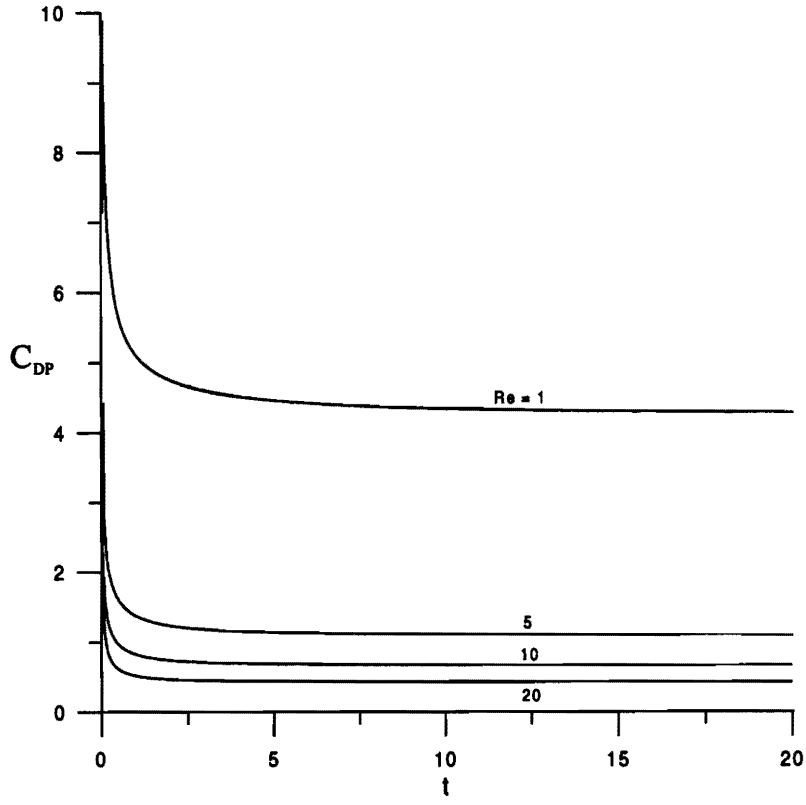

Figure 5. The Time Development of the Pressure Component of Drag.

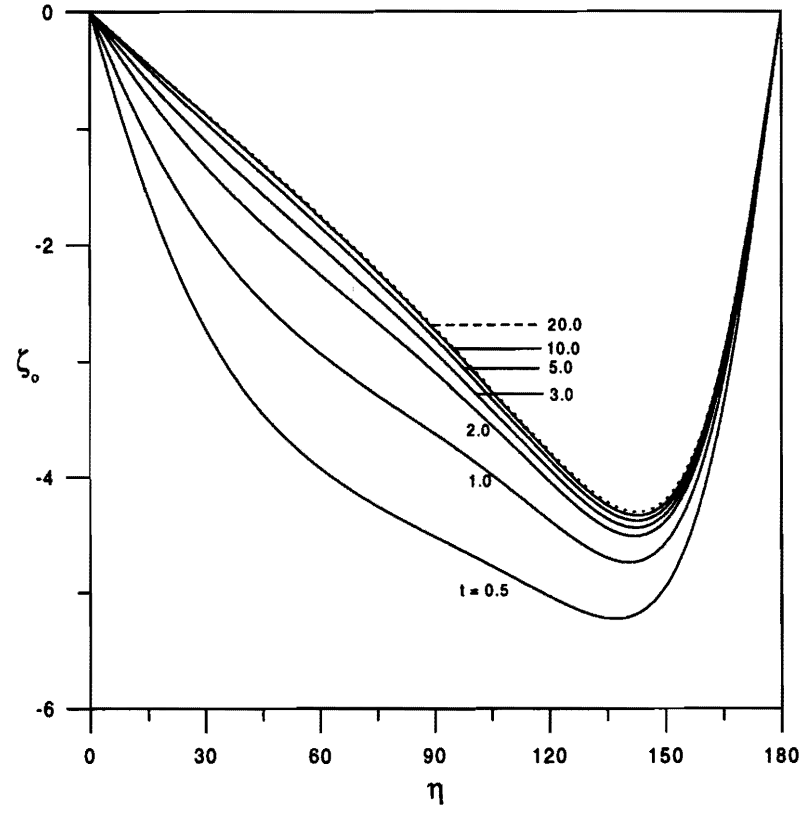

Figure 6. The Time Development of Surface Vorticity for the case Re = 20.

Figure 4 shows the time development of C_D while Figure 5 shows the time development of C_{DP} for Re = 1.0, 5.0, 10.0, and 20.0. The computations were terminated at t = 20.0 at which a steady state condition was assumed. Higher Re cases tend to steady state faster than those of low Re. The time variation of the surface vorticity and pressure distributions for the case Re = 20 are shown in Figures 6 and 7. Figure 6 shows that the maximum surface vorticity, ζ_o, occurs near $\eta = 140°$. At small times, $|\zeta_o|$ is high and decreases with the increase of t because of the growth of the boundary layer thickness. The same trend was reported earlier for the case of a sphere by Dennis and Walker [8]. Figure 7 shows the time development of the surface pressure distribution for the same case. The maximum pressure is at the forward stagnation point $(\eta = 180°)$. The surface vorticity distributions at large times (steady cases) are shown in Figure 8. The corresponding surface pressure distributions are shown in Figure 9. Figure 8 shows that flow separation does not occur for this range of low Re.

The flow structure near the spheroid surface at large time is shown in Figures 10(a) and 10(b) for the cases of Re = 20, b/a = 0.6, and Re = 86.6, b/a = 0.5, respectively. The right half of the figures shows streamlines while the left half shows equi-vorticity lines. As mentioned earlier, no separation is observed for this low Re number.

ACKNOWLEDGMENT

The authors wish to acknowledge the support of King Fahd University of Petroleum and Minerals.

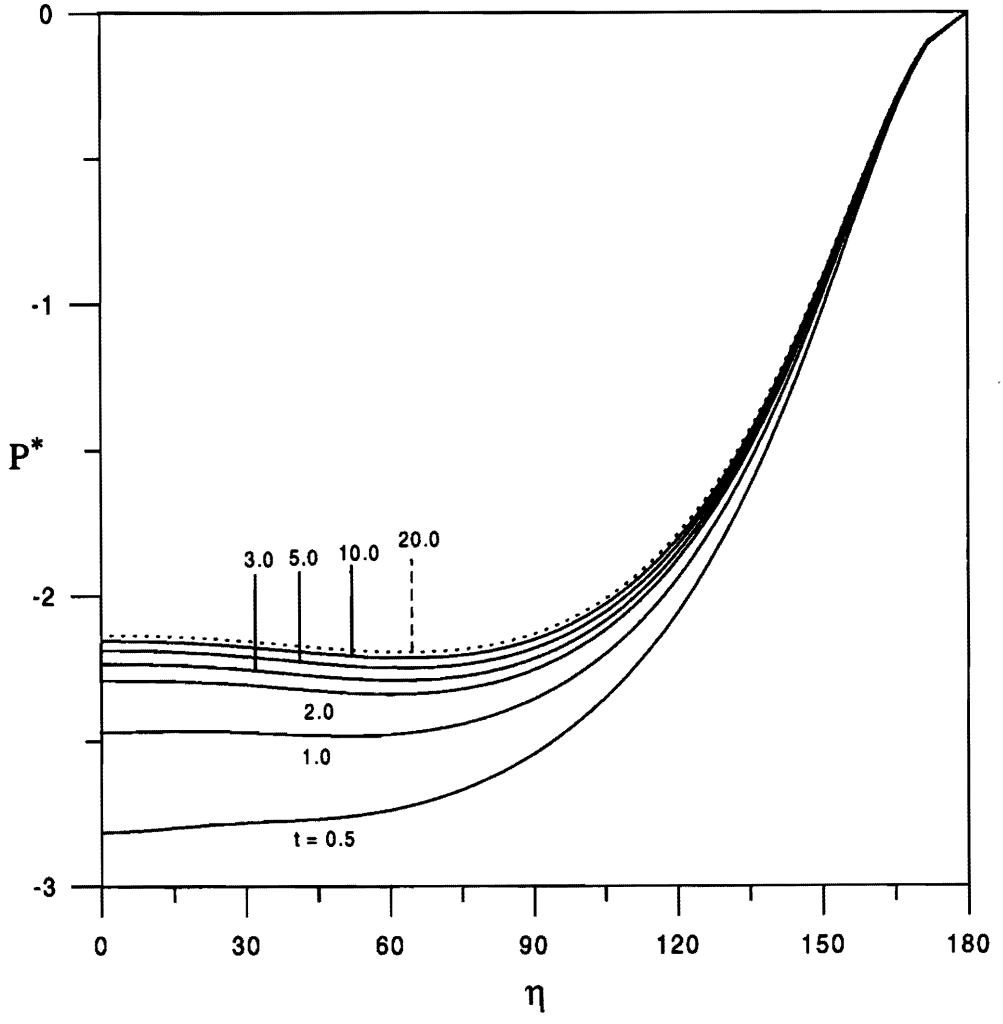

Figure 7. The Time Development of Dimensionless Pressure for the Case Re = 20.

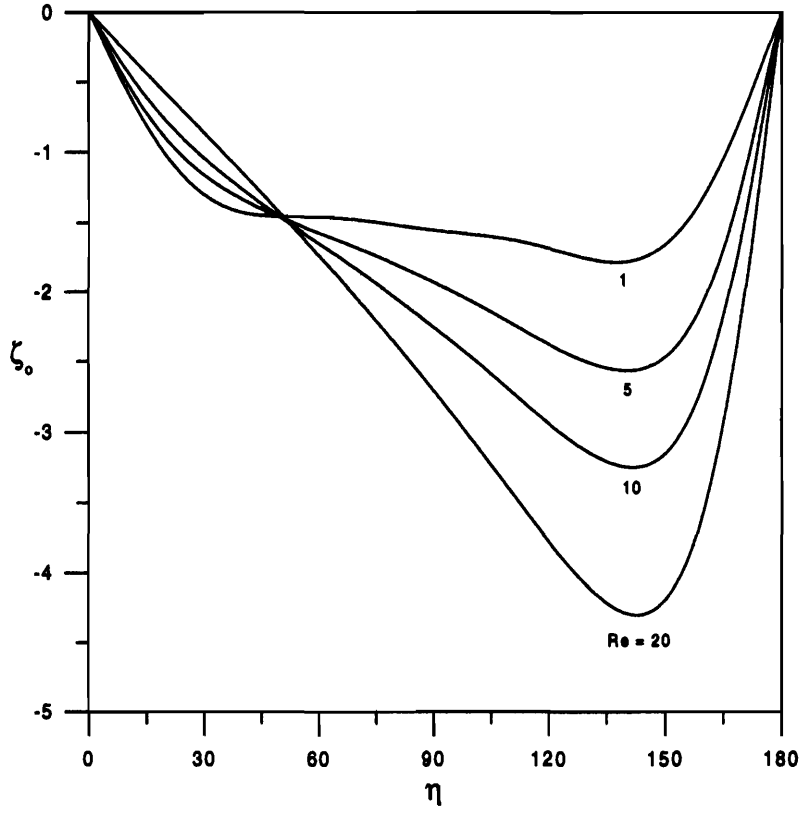

Figure 8. Comparisons of Surface Vorticity at Large Time.

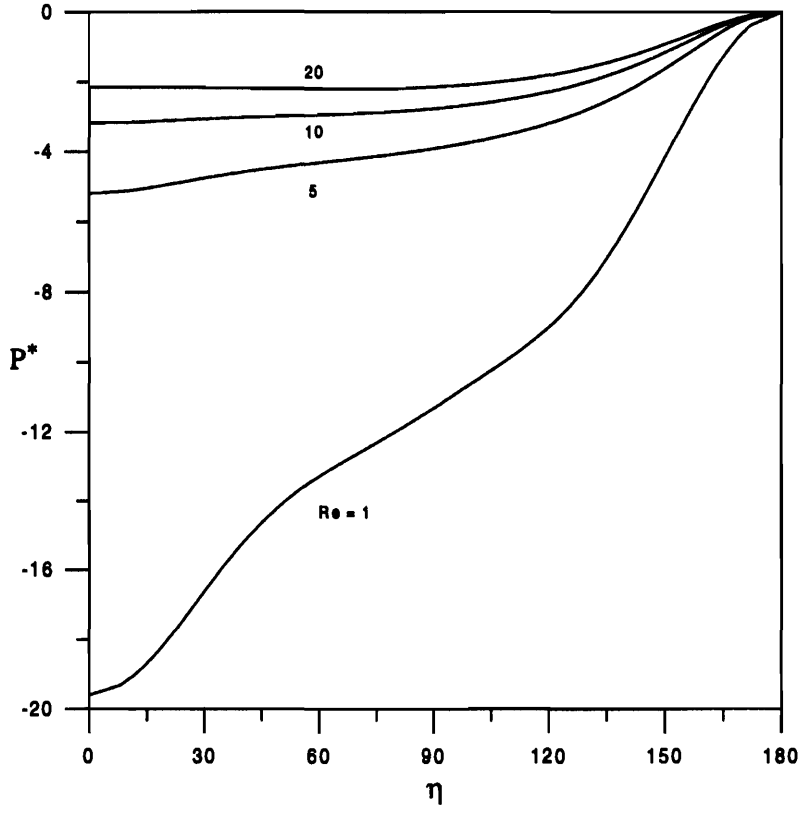

Figure 9. Comparisons of Dimensionless Pressure at Large Time.

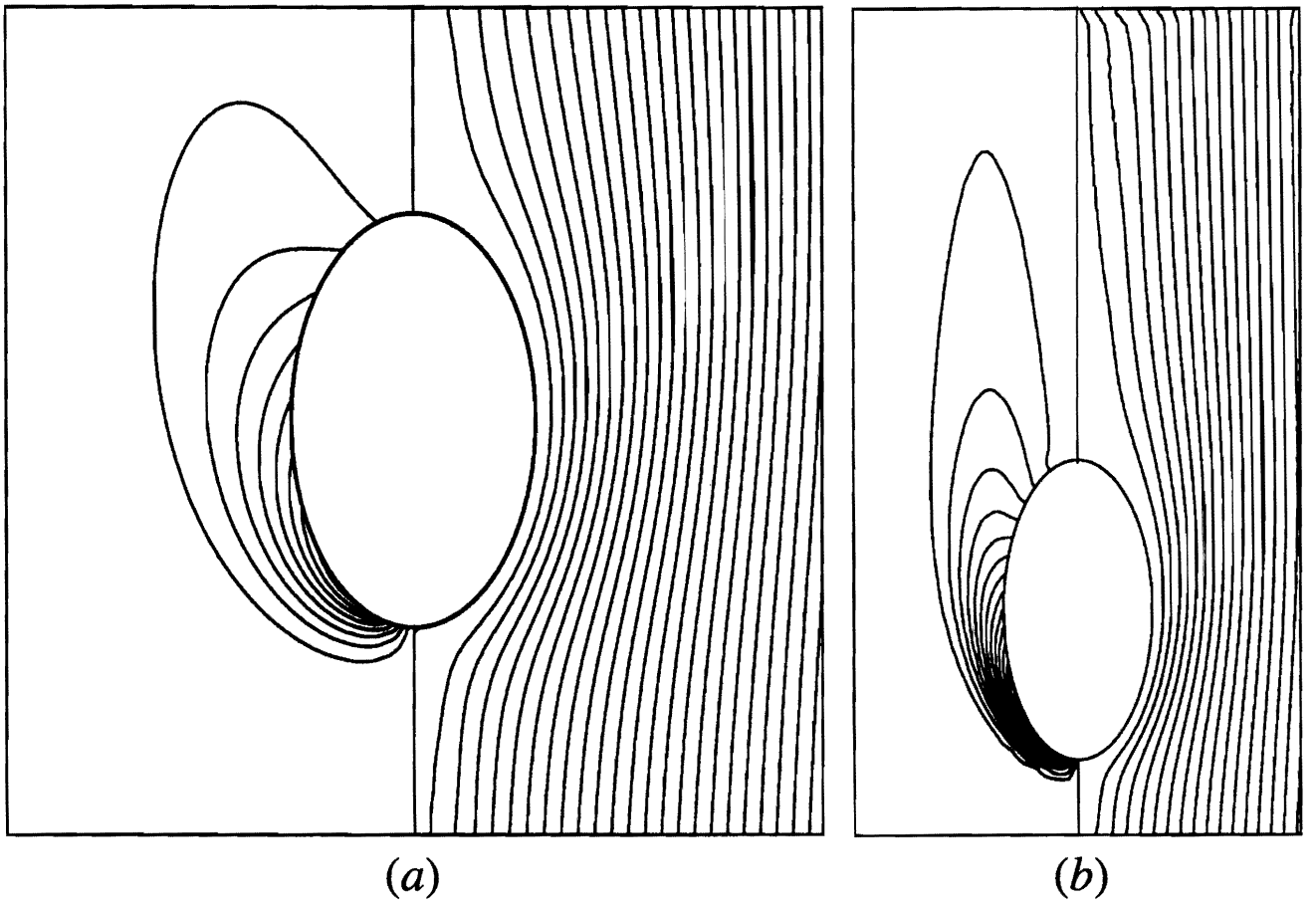

Figure 10(a) *Streamline and Equi-Vorticity Patterns for the Case* Re = *20;*
(b) *Streamline and Equi-Vorticity Patterns for the Case* Re = *86.6.*

REFERENCES

[1] L.E. Payne and W.H. Pell, "The Stokes Flow Problem for a Class of Axially Symmetric Bodies", *J. Fluid Mech.* **7** (1960), pp. 529–549.

[2] D.R. Breach, "Slow Flow Past Ellipsoids of Revolution", *J. Fluid Mech.*, **10** (1961), pp. 306–314.

[3] G.G. Stokes, "On the Effect of the Internal Friction of Fluids on Pendulums", *Trans. Camb. Phil. Soc.*, **9** (1851), p. 8.

[4] C.W. Oseen, "Uber die Stokes'sche Formel und uber eine verwandte Aufgabe in der Hydrodynamik", *Ark f. Math.Astron. och Fys.*, **6** (1910), p. 29.

[5] R.P. Kanwal, "Rotary and Longitudinal Oscillations of Axi-Symmetric Bodies in a Viscous Fluid", *Q.J. Mech. Appl. Math.*, **8** (1995), pp. 146–163.

[6] R.Y.S. Lai and L.F. Mockros, "The Stokes-Flow on Prolate and Oblate Spheroids During Axial Translatory Accelerations", *J. Fluid Mech.*, **52** (1972), pp. 1–15.

[7] C.C. Chang, B. Liou, and R. Chern, "An Analytical Study of Axisymmetric Flow Around Spheroids", *J. Fluid Mech.*, **334** (1992), pp. 219–246.

[8] S.C.R. Dennis and J.D.A.Walker, "Numerical Solution for Time-Dependent Flow Past an Impulsively Started Sphere", *The Physics of Fluids*, **15(4)** (1972), pp. 517–525.

Paper Received 15 February 1997; Revised 16 September 1997; Accepted 19 October 1997.